pH control for enhanced reductive bioremediation of chlorinated solvent source zones

Clare Robinson[1,2,#], D. A. Barry[1], Perry L. McCarty[3], Jason I. Gerhard[2,4] and Irina Kouznetsova[4]

[1]*Laboratoire de technologie écologique, Institut de sciences et technologies de l'environnement, Station No. 2, Ecole Polytechnique Fédérale de Lausanne, CH-1015 Lausanne, Switzerland*

[2]*Now at: Department of Civil and Environmental Engineering, University of Western Ontario, London, N6A 5B9 Canada*

[3]*Department of Civil and Environmental Engineering, Stanford University, Stanford, CA 94305-4020 USA*

[4]*Institute for Infrastructure and Environment, University of Edinburgh, Edinburgh, EH9 3JL UK.*

Revised version submitted to *Science of the Total Environment* on 18th March 2009

[#] Author to whom correspondence should be addressed. Tel.: +41 21 693-2757; Fax: +41 21 693-5670; E-mail addresses: clare.robinson@epfl.ch, andrew.barry@epfl.ch, pmccarty@stanford.edu, j.gerhard@ed.ac.uk, irina.kouznetsova@ed.ac.uk.

Abstract

Enhanced reductive dehalogenation is an attractive treatment technology for in situ remediation of chlorinated solvent DNAPL source areas. Reductive dehalogenation is an acid-forming process with hydrochloric acid and also organic acids from fermentation of the electron donors typically building up in the source zone during remediation. This can lead to groundwater acidification thereby inhibiting the activity of dehalogenating microorganisms. Where the soils' natural buffering capacity is likely to be exceeded, the addition of an external source of alkalinity is needed to ensure sustained dehalogenation. To assist in the design of bioremediation systems, an abiotic geochemical model was developed to provide insight into the processes influencing the groundwater acidity as dehalogenation proceeds, and to predict the amount of bicarbonate required to maintain the pH at a suitable level for dehalogenating bacteria (i.e., > 6.5). The model accounts for the amount of chlorinated solvent degraded, site water chemistry, electron donor, alternative terminal electron-accepting processes, gas release and soil mineralogy. While calcite and iron oxides were shown to be the key minerals influencing the soil's buffering capacity, for the extensive dehalogenation likely to occur in a DNAPL source zone, significant bicarbonate addition may be necessary even in soils that are naturally well buffered. Results indicated that the bicarbonate requirement strongly depends on the electron donor used and availability of competing electron acceptors (e.g., sulfate, iron(III)). Based on understanding gained from this model, a simplified model was developed for calculating a preliminary design estimate of the bicarbonate addition required to control the pH for user-specified operating conditions.

Keywords: reductive dehalogenation, dechlorination, alkalinity, trichloroethene, bicarbonate, electron donor, DNAPL, PHREEQC

1. Introduction

Chlorinated ethenes, such as tetrachloroethene (PCE) and trichloroethene (TCE), are among the most persistent and hazardous groundwater contaminants (National Research Council, 2004; Rivett et al., 2005). Enhanced reductive dehalogenation is widely used for the in situ remediation of chlorinated ethene plumes and is now recognized as a promising technology for DNAPL source areas (McCarty, 1997; Ellis et al., 2000; Major et al., 2002; Yang and McCarty, 2002; AFCEE, 2004). Here, biodegradation is achieved by stimulating the activity of dehalogenating bacteria – e.g., *Dehalococcoides* (Major et al., 2002; Loffler and Edwards, 2006), *Sulfurospirillum multivorans* (Neumann, 1994; Amos et al., 2007; Amos et al., 2008), *Dehalobacter restrictus* (Schumacher and Holliger, 1996) – through the addition of an electron donor. Recent studies have indicated that remediation in the proximity of the source zone, rather than dilute plume dehalogenation, results in more efficient degradation due to enhanced rates of solvent dissolution and thus reduction in the longevity of the DNAPL plume (Yang and McCarty, 2000; Amos et al., 2008).

Although increased understanding of dehalogenating bacteria and suitable electron donors has led to more rapid dehalogenation rates (Carr and Hughes, 1998; Aulenta et al., 2006), complete dehalogenation to ethene is still often hindered at many sites due to, for example, inadequate electron donor supply (Yang and McCarty, 2002; Aulenta et al., 2006; Loffler and Edwards, 2006; Aulenta et al., 2007), high concentrations of alternative electron acceptors (e.g., sulfate) (Hoelen and Reinhard, 2004; Heimann et al., 2005; Aulenta et al., 2006), insufficient contact time (Da Silva et al., 2006), absence of suitable consortia of dehalogenating bacteria (Loffler and Edwards, 2006; Amos et al., 2007) and development of low groundwater pH (Cope and Hughes, 2001; Adamson et al., 2004; McCarty et al., 2007). Reductive dehalogenation occurs in a step-wise manner converting PCE to TCE to dichloroethene (DCE) to vinyl chloride (VC), and finally to ethene. Each step involves the removal of one chlorine atom from the chlorinated ethene molecule, giving rise to hydrochloric acid (HCl) production. The combination of this strong acid and the build-up of organic acids formed during electron donor fermentation can result in groundwater acidification (Adamson et al., 2004; AFCEE, 2004; Chu et al., 2004; Amos et al., 2008). The groundwater pH is typically strongly controlled by the dissolved carbonate equilibria,

$$CO_3^{2-} + 2H^+ = HCO_3^- + H^+ = CO_2 + H_2O. \quad (1)$$

The acid formed during dehalogenation reacts with bicarbonate (HCO_3^-) to produce carbon dioxide (CO_2). In aquifers, CO_2 is not readily released to the atmosphere, and the increase in dissolved CO_2 coupled with the decrease in HCO_3^- depresses the pH further. This is evident from the HCO_3^-/CO_2 equilibrium expression:

$$\frac{[H^+][HCO_3^-]}{[CO_2]} = K = 10^{-6.3}, \quad (2)$$

where K is the equilibrium constant and the bracketed quantities denote molar aqueous concentrations.

Laboratory studies have demonstrated that the optimal pH range for dehalogenating microorganisms is 6.8 – 7.8 (Middeldorp et al., 1999; Cope and Hughes, 2001; AFCEE, 2004) and, correspondingly, that low pH leads to reduced dehalogenation rates (Cirpka et al., 1999; Adamson et al., 2004). Acidic conditions inhibit, in particular, the dehalogenation of the lesser chlorinated ethenes (Christ et al., 2005). Where pH drops are expected or observed, an alkalinity source such as sodium or potassium bicarbonate can be added to raise and/or neutralize the pH (AFCEE, 2004; Payne et al., 2006). Other buffers such as sodium carbonate or hydroxide tend to provide unstable pH control, while lime (CaO) addition is likely to lead to calcite ($CaCO_3$) precipitation and subsequent aquifer clogging (McCarty et al., 2007). Bicarbonate addition offsets the impact of the higher dissolved CO_2 concentrations produced from dehalogenation. With recent developments (e.g., the availability of increasingly effective bacterial consortia, electron donors, injection strategies, etc.) allowing for more complete and rapid dehalogenation, more acidity is generated and thus there is an increasing need for pH control strategies. Furthermore, acidification is more likely during DNAPL source area bioremediation due to the higher mass of chlorinated ethenes dehalogenated compared with dilute plume bioremediation.

The two main issues associated with the design of pH control strategies are (1) the amount of bicarbonate addition needed as dehalogenation proceeds, and (2) how best to deliver this bicarbonate to the DNAPL source area. This study focuses on the first issue. McCarty et al. (2007) calculated the amount of reductive dehalogenation likely to occur prior to pH inhibition for a range of electron donors and initial bicarbonate alkalinities. While they demonstrated that bicarbonate addition is likely required for effective dehalogenation in source areas, the study raised a number of questions including the influence of mineralogy, competing terminal electron-accepting processes (TEAPs) and gas release on the acidity generated and the subsequent amount of bicarbonate required to maintain the pH at a suitable level for dehalogenating bacteria. Quantitative responses to these questions would clearly benefit detailed bioremediation system design.

This paper presents an abiotic geochemical model to address these issues. The model is implemented through the geochemical program PHREEQC version 2.15 (Parkhurst and Appelo, 1999). The model is first described and simulation results for conditions pertinent to a typical remediation site are presented. The model accounts for the amount of dehalogenation, site water chemistry, electron donor, potential gas release, use of acetate as an electron donor, competing TEAPs and the precipitation and dissolution kinetics of common minerals. Following this, the paper explores the main factors influencing the bicarbonate requirements: (1) mineralogy, (2) electron donor, (3) minimum design pH, (4) acetate oxidization, and (5) competing TEAPs. Based on insight gained from these analyses, a simplified model is presented that may be used to calculate a preliminary estimate of the bicarbonate addition required once the minimum design pH is reached.

2. Process understanding and model development

Enhanced reductive dehalogenation is a complex, microbially mediated process. Rather than simulating the suite of biological reactions influencing dehalogenation, the objective here was to develop an abiotic geochemical model focused on predicting the acidity generated during dehalogenation and the bicarbonate required for pH control. The main processes influencing the groundwater pH as dehalogenation proceeds are presented in Fig. 1. pH control is achieved by balancing the acidity and alkalinity perturbations using bicarbonate amendment. In this section, the various processes given in Fig. 1 are described.

Acidity is generated directly from dehalogenation (i.e., HCl) and from the by-products of electron donor fermentation. The model assumes that the remediation scheme will degrade a given amount of chlorinated ethenes according to:

$$R\text{-}Cl + H_2 = R\text{-}H + HCl. \qquad (3)$$

By simulating the reduction of a generic chlorinated ethene compound (R-Cl), the results can be interpreted regardless of which chlorinated ethene is actually reduced. That is, Cl production is used to quantify the amount of dehalogenation. While the H_2 required for dehalogenation in (3) can be directly injected into the aquifer, more often an organic, fermentable electron donor is used. The acidity generated from fermentation depends on the specific electron donor used, with each producing different amounts of acetate and carbonate species (McCarty et al., 2007). Fermentation reactions for common donors based on standard biochemical pathways are given in Table 1. While acetate and carbonate species increase acidity, the presence of sodium associated with an electron donor (e.g., sodium lactate and formate) reduces this acidity because bicarbonate is formed upon fermentation rather than carbon dioxide (McCarty et al., 2007) (Fig. 1).

Acetate generated from electron donor fermentation can also serve as an electron donor for conversion of PCE and TCE to DCE, but not directly, if at all, in the conversion of DCE and VC (Dolfing and Tiedje, 1991; Krumholz et al., 1996; Sharma and McCarty, 1996; Loffler et al., 2000; Sung et al., 2003; Lee et al., 2007). With R-Cl representing PCE or TCE, the dehalogenation reaction with acetate as the electron donor is:

$$4R\text{-}Cl + CH_3COOH + 2H_2O = 4R\text{-}H + 2CO_2 + 4HCl. \qquad (4)$$

This process not only reduces the overall electron donor requirements and concentration of acetic acid, but also leads to the production of CO_2, thus shifting the carbonate equilibrium in (2). There is also some evidence that acetate might be fermented to H_2

and CO_2, and the H_2 produced might then be used for dehalogenation of DCE and VC (He et al., 2002). A parameter, *p*, is used in the model to specify the fraction of acetate produced from donor fermentation that is subsequently used as an electron donor.

Not all the H_2 and acetate produced from fermentation are used for dehalogenation as dehalogenating bacteria must compete for these electron donors with other microbial populations such as denitrifiers, iron and sulfate reducers and methanogens (Table 2). In addition to these TEAPs increasing the amount of electron donor fermented, and thus the acidity generated for a given level of dehalogenation, each TEAP adds a different amount of alkalinity per mol of H_2 consumed (Table 2). In the presence of multiple electron acceptors, species are generally reduced in order of thermodynamic preference: oxygen reduction > nitrate reduction > iron(III) reduction > dehalogenation > sulfate reduction > methanogenesis (Loffler et al., 1999; Curtis, 2003). While this sequence, and thus the fraction of H_2 directed to dehalogenation, may be predicted based on thermodynamic considerations (Gibbs free energy of reaction, $\Delta G_r{}^\circ$), competition also depends on microbial populations and specific field conditions (Dolfing and Janssen, 1994; Jakobsen and Postma, 1999; Loffler et al., 1999; Curtis, 2003). Methanogenesis is not included in the model as this TEAP is assumed to be inhibited by the low H_2 concentrations and high chlorinated solvent concentrations in the source zone (Yang and McCarty, 2000). Furthermore, oxygen and nitrate reduction are not considered as these electron acceptors must be reduced before dehalogenating conditions can be induced (AFCEE, 2004). Sulfate and iron(III) reduction however often occur concomitantly with dehalogenation and thus these electron acceptors compete for H_2 (AFCEE, 2004; Heimann et al., 2005; Aulenta et al., 2007). As the proportion of H_2 used for dehalogenation is not known a priori due to the complexity of the microbial processes, the model assumes that at least a fraction (f_{min}) of the H_2 generated by electron donor fermentation is used for dehalogenation with the remainder (1 - f_{min}) used for iron(III) and sulfate reduction (Fig. 1).

For arbitrary *f*, the dehalogenation reaction (3) and fermentation reaction for each electron donor can be combined giving an overall stoichiometry for dehalogenation (Table 1). Our modeling approach is to follow this overall dehalogenation reaction as it progresses in reaction steps. The sequence of calculations performed at each step is outlined in Fig. 2. In the simulations presented, 40 mM of chlorinated ethene compound (R-Cl) are assumed to degrade over 100 d (the residence time for water to flow through a hypothesized DNAPL source zone). This residence time is divided equally into 500 reaction steps. Although complete dehalogenation of TCE at its solubility limit (7.6 mM) to ethene corresponds to only 22.8 mM of chlorinated ethene compound degraded, it is envisaged that with effective remediation scheme design (i.e., design that leads to favorable dehalogenating conditions in the source zone including the presence of a suitable electron donor and consortia of dehalogenating bacteria, and neutral pH conditions), the amount of dehalogenation occurring may extend beyond this with more PCE and TCE dissolving into solution as transformation to lesser chlorinated compounds proceeds.

For each reaction step, *f* is first calculated based on the availability of iron(III) and sulfate. *f* is set to an assumed minimum value (f_{min}) when these electron acceptors are in excess (i.e., 0.2 (AFCEE, 2004)). As iron(III) and sulfate become limited, *f* is calculated such that only the H_2 required to reduce the iron(III) and sulfate available will be produced in the overall dehalogenation reaction. It follows that when sulfate and iron oxides are depleted, *f* is set to unity and all H_2 generated from fermentation goes to dehalogenation. With *f* calculated, 40/500 mM of R-Cl (total mM of R-Cl to degrade/number of time steps) then reacts according to the overall dehalogenation and fermentation reaction for the selected electron donor (Table 1). Following this, PHREEQC equilibrates the solution and, in doing so, the nonchlorinated electron acceptors consume the surplus H_2 produced in the reaction. The sequence by which iron(III) and sulfate are consumed when the solution is equilibrated is based on thermodynamics and therefore at each step the available iron(III) is reduced in preference to sulfate.

As the solution is speciated, minerals are allowed to dissolve and/or precipitate. Carbonate minerals, in particular calcite, are typically the main source of natural alkalinity. Other minerals such as silicates may provide important buffering capacity (Appelo and Postma, 2005); however, unlike carbonate minerals that dissolve rapidly, these minerals are typically slow to equilibrate and thus their buffering capacity is strongly kinetically-controlled. The dissolution and reduction of iron oxides (e.g., goethite [FeOOH], ferrihydrite [$Fe(OH)_3$]) also adds alkalinity whilst consuming H_2 (Table 2, Fig. 1). Although the dissolution and subsequent reduction of iron oxides is also kinetically controlled, the process is often enhanced by iron-reducing bacteria (Maurer and Rittmann, 2004). Finally, iron sulfides, in particular acid volatile sulfide (FeS), may precipitate rapidly following sulfate and iron(III) reduction (Rickard, 1995). The direct precipitation of iron sulfide adds acidity according to:

$$Fe^{2+} + H_2S = FeS\,(s) + 2H^+. \quad (5a)$$

However, when the overall reaction for iron sulfide precipitation, including sulfate and iron(III) reduction is considered:

$$FeOOH(s) + 4.5H_2 + SO_4^{2-} = FeS(s) + 2OH^- + 4H_2O, \quad (5b)$$

it is evident that the overall reduction and precipitation process adds alkalinity to the solution. Although cation exchange can also influence sediment's natural buffering capacity, simulations indicate that these effects are only likely to be significant when the pH drops below approximately 4.5. Thus this process is not included in the model.

As the solution is speciated, a gas phase is also allowed to form and gas is released if the sum of the partial pressures of all the gases present (CO_2, CH_4, N_2, H_2O, H_2, H_2S, O_2) exceeds a given total pressure. This total pressure corresponds to a given depth below the water table, assuming that the water flow is predominantly horizontal. The release of CO_2(g) influences the groundwater acidity as indicated in (2).

Finally, upon speciation of the solution, the pH is calculated (Fig. 2). Once the pH decreases to the microbial inhibition level (pH = 6.5 in these simulations), iterations are performed such that sufficient bicarbonate is added to maintain this pH (i.e., in Fig. 1 the acidity and alkalinity added must be equal). This procedure (Fig. 2) is repeated until the total number of steps is reached and thus the required amount of R-Cl is degraded. In the simulations presented in this paper, sodium bicarbonate ($NaHCO_3$) is used as the bicarbonate source; however the results are insensitive to whether $NaHCO_3$ or another bicarbonate salt such as potassium bicarbonate ($KHCO_3$) is added. Addition of calcium bicarbonate however is not recommended as it will likely lead to calcite precipitation and aquifer clogging in the remediation zone.

3. Model setup for base conditions

The model was first setup to simulate conditions pertinent to a typical remediation site. Sensitivity analyses were then performed on this base case. The operating and design parameters used are as follows:

- Initial solution composition is specified using typical values of the major constituents at contaminated chlorinated solvent sites (Table 3) (AFCEE, 2004).
- 40 mM of chlorinated ethene compound (R-Cl) degrades over 100 d.
- The inhibition level for bacteria and therefore minimum design pH = 6.5.
- Linoleic acid is used as the electron donor. This is a typical major component of water insoluble electron donors such as emulsified vegetable oil which are increasingly being used due to their slow controlled release rate (AFCEE, 2004; Long and Borden, 2006).
- Acetate is not used as an electron donor ($p = 0$).
- $f_{min} = 0.2$. Design factors for f commonly used to calculate the quantity of electron donor required for bioremediation are of the order of 0.2 to 0.5 (AFCEE, 2004).
- An excess of calcite ($CaCO_3$) is present and in equilibrium with the solution, i.e., saturation index (SI) = 0.
- Mass fraction of iron oxides in the soil is 7.5 wt % (3.4 mol kg of water^{-1}). This mass fraction is based on the mineralogy at a contaminated chlorinated solvent site currently undergoing enhanced bioremediation. The dissolution of iron oxides is controlled by the rate (R, mol m^{-3} s^{-1}):

$$R = k\frac{A_0}{V}\left(\frac{m}{m_0}\right)[H^+]^{0.45}, \quad (6)$$

where k (mol m^{-2} s^{-1}) is the rate constant, A_0 (m^2) is the initial surface area of iron oxides, V (m^3) is the solution volume, m_0 (mol) is the initial moles and m (mol) is the undissolved moles of iron oxides (Appelo and Postma, 2005). The specific mineral surface area = 55 m^2 g^{-1} (Roden, 2006) and k is $10^{-10.2}$ mol m^{-2} s^{-1}. The latter value assumes that 10% of the iron oxides are ferrihydrite (freshly precipitated) with the remainder being stable, well-crystallized goethite (Appelo and Postma, 2005).

- Iron sulfide is initially absent but it is allowed to precipitate if the solution becomes oversaturated (SI > 0).
- A gas phase is allowed to form once the sum of the partial pressure of all gases present exceeds 1.5 atm. This total pressure is equivalent to a location approximately 5 m below the watertable. The initial partial pressure for all the gases is negligible except N_2 for which the partial pressure is set at 0.79 atm (Amos and Mayer, 2006), and CO_2 for which the partial pressure is fixed by specification of the initial solution alkalinity and pH (Table 3).

4. Results

4.1 Base conditions

For the base conditions it is predicted that pH control is necessary when more than ~4.5 mM of chlorinated ethene equivalents (Cl^-) are produced from dehalogenation (Fig. 3a). Although there is an excess of calcite present, the results indicate that its buffering capacity is not sufficient to maintain the pH above 6.5. The dissolution of calcite is limited by its solubility rather than kinetic constraints, and only 0.037 mol of calcite are predicted to dissolve for 40 mM of dehalogenation (- - in Fig. 3e). Although calcite is not able to supply sufficient pH control for sustained dehalogenation, its buffering capacity is still important as simulations indicate that if calcite is initially absent, the pH reaches 6.5 after only 0.8 mM of dehalogenation compared to after 3.6 mM of dehalogenation if calcite is present (Fig. 3a). It should be noted that for the simulation without bicarbonate addition, once the pH drops below 6.5 the results are theoretical because as the acidity increases the bacteria would become inhibited and thus, in reality, dehalogenation would stall.

For the conditions simulated, the total bicarbonate required to maintain the pH at 6.5 along with dehalogenation of 40 mM of chlorinated ethene equivalents is ~197 mM (Fig. 3b). This total requirement is the sum of the initial solution alkalinity plus the bicarbonate that needs to be added. The initial alkalinity affects the extent of dehalogenation likely to occur prior to microbial inhibition, however, once the design pH is reached, the total bicarbonate required to maintain that pH as dehalogenation proceeds is the same. With f_{min} = 0.2, sulfate is depleted after 10.9 mM of dehalogenation (Fig. 3c). In contrast, iron(III) reduction (rate controlled) and iron sulfide precipitation continue as dehalogenation proceeds (Fig. 3e). Once sulfate is depleted, f is automatically adjusted to ~0.88 such that the H_2 directed away from dehalogenation matches that required for iron(III) reduction, the sole remaining nonchlorinated TEAP when methanogenesis is inhibited by high PCE or TCE concentrations. The availability of iron(III) and therefore the adjusted f, depends on the iron oxide dissolution rate (6). When sulfate is present, the bicarbonate addition required to match the acidity generated is ~7.5 mM per mM of dehalogenation. This requirement reduces to ~4.9 mM per mM of dehalogenation after sulfate has been depleted (Fig. 3b). The decrease in the bicarbonate requirement is primarily due to less acetic acid produced per mM of dehalogenation as f increases (Fig. 3d). The effects however are complicated because sulfate and iron(III) reduction and iron sulfide precipitation also influence the alkalinity (Table 2 and Equation 5). These effects are discussed further in Section 4.6.

Due to the common ion effect, when bicarbonate is added the build-up of carbonate species leads to a net precipitation of calcite rather than dissolution (Fig. 3e).

The calcite that dissolves as the pH decreases from 7 to 6.5 rapidly re-precipitates upon bicarbonate addition. However, calcite precipitation is not significant as dehalogenation and bicarbonate addition continue. This result reveals that the amount of bicarbonate required does not depend on the amount of calcite present.

The model predicts that, for the conditions simulated, the build-up of dissolved CO_2 accompanying dehalogenation and bicarbonate addition leads to gas bubble formation after 9.9 mM of dehalogenation (Fig. 3f). This is when the partial pressure of all the gases sums to 1.5 atm. Whilst N_2 is the dominant species when the gas phase forms (initial partial pressure = 0.79), the gas composition changes as dehalogenation proceeds with CO_2(g) becoming the major component. Due to the shift in the carbonate equilibria (2) as CO_2(g) is released, the bicarbonate requirement is reduced from ~4.9 mM when the gas phase initially forms to ~2.6 mM per mM of dehalogenation as dehalogenation and CO_2(g) release continues (— in Fig. 3b). If a gas phase is not permitted to form, the amount of bicarbonate required per additional mol of dehalogenation is constant (- - in Fig. 3b).

4.2 Influence of mineralogy

Dissolution, reduction and precipitation kinetics for common crystalline minerals (calcite, iron oxides, gypsum, anorthite, K-feldspar, albite, chlorite and illite) were included in the model to identify minerals likely to influence the sediment buffering capacity over the timescale for groundwater to flow through the treatment zone (i.e., 100 d). For all minerals except gypsum, the rate expressions implemented and rate constants adopted were based on Appelo and Postma (2005). For gypsum, the rate expression of Singh and Bajwa (1990) was employed. The simulation revealed that calcite and gypsum dissolution, and iron oxide reduction are the main crystalline mineral processes likely to significantly influence the soil's natural buffering capacity over this timescale. The amounts of each mineral that dissolved for 40 mM of dehalogenation with no bicarbonate added are provided in Table 4. The initial amounts present are based on the mineralogy at a contaminated chlorinated solvent site currently undergoing enhanced bioremediation. Gypsum was absent in the contaminated layer at this particular site, but included here to examine its potential for dissolution. Simulations demonstrated that iron oxide reduction and dissolution is strongly rate controlled, while calcite and gypsum dissolution is of the order of hours and therefore these minerals can be considered to be in equilibrium (SI = 0). Sulfate containing minerals such as gypsum can influence the bicarbonate requirement due to the buffering effects of sulfate reduction. The influence of the sulfate availability is examined in Section 4.6.1 and the influence of the iron oxide reduction rate is discussed in Section 4.6.2. While silicate minerals are common and can provide important natural buffering, the simulation indicated that, unless the residence time of water traveling through the treatment zone is greater than approximately one year, the dissolution kinetics for these minerals are too slow to influence the acidity response. Of the silicate minerals considered, anorthite dissolution was the fastest, however for 40 mM of dehalogenation occurring over 100 d, the quantity of anorthite predicted to dissolve was two orders of magnitude lower than for calcite (Table 4).

4.3 Influence of electron donor selection

The acidity response and bicarbonate requirements for different electron donors are presented in Fig. 4. The operating conditions for these simulations, with the exception of the electron donor used, are identical to the base case (Section 3). As discussed by McCarty et al. (2007), the net acidity generated is directly related to the relative amounts of acetate, carbonate species, and in some cases sodium associated with the fermentation process (Table 1). The extent of dehalogenation predicted to occur prior to pH inhibition and the amount of bicarbonate required per mM of dehalogenation for each electron donor with $f = 0.2$ (sulfate and iron(III) available) and $f = 0.88$ (sulfate exhausted and f adjusted based on iron oxide dissolution rate) are shown in Table 5. Note that lactic acid and glucose generate the same by-products per mol of H_2 (Table 1) and therefore have the same acidity response and bicarbonate requirements. Although the pH drop is greatest for these donors (Fig. 4a), the bicarbonate requirement is largest for butyric acid (Fig. 4b). This is because lactic acid and glucose fermentation adds 0.5 mol of acetate species and 0.5 mol of carbonate species per mol of H_2, compared with butyric acid that adds one mol of acetate species and no carbonate species. The effects of sodium in reducing the acidity generated are evident in comparing the results for lactic acid to those for sodium lactate. As expected, for all electron donors the release of CO_2 significantly reduces the bicarbonate requirements as evident in comparing Fig. 4b and Fig 4c. For all donors, with $f_{min} = 0.2$, sulfate is depleted after 10.9 mM of dehalogenation and as f switches to 0.88 the additional bicarbonate needed per mM of dehalogenation decreases (Table 5, Fig. 4b,c).

Of all the electron donors considered, only formate does not require pH buffering, confirming the observation of McCarty et al. (2007) that it is an excellent choice in terms of pH control. This is because acetic acid is not produced and the sodium released is able to neutralize the HCl produced from dehalogenation. For the conditions simulated, the use of formate causes the pH to only decrease to 6.6 for 40 mM of dehalogenation and therefore no bicarbonate addition is required (Fig. 4). When sulfate is present during formate fermentation, the pH increases indicating that the alkalinity added to the solution from sulfate and iron(III) reduction is greater than the acidity generated from the overall dehalogenation and fermentation reaction. Note that the results show an initial pH drop (Fig. 4a, dehalogenation < 2.5 mM). This is associated with the rapid precipitation of calcite. However the calcium concentration rapidly decreases, as does the rate of calcite precipitation, and this is accompanied by an increase in pH. Once sulfate is depleted and f switches to 0.88, the acidity generated from the overall dehalogenation reaction exceeds the alkalinity added from iron(III) reduction and the pH gradually decreases (Fig. 4a).

This comparison of electron donors assumes that dehalogenation rates and competition for H_2 are independent of the specific electron donor used. In a detailed field design, it may be necessary however to account for the characteristics of the electron donor used. While we have adopted f_{min} = 0.2 for all electron donors, donors such as glucose, ethanol, methanol, lactic acid and lactate ferment very rapidly and therefore may have lower H_2 efficiencies of consumption (Fennell et al., 1997; Yang and McCarty, 2002; AFCEE, 2004). Furthermore, some donors can also ferment via alternative pathways that result, for example, in the production of propionate (Aulenta et al., 2007). Both of these effects would likely increase the acidity generated and thus bicarbonate requirements. A benefit of linoleic acid (vegetable oil emulsions), the donor used for the base case, is that it only oxidizes under a low H_2 partial pressure and therefore has a high efficiency of consumption by dehalogenating microorganisms (AFCEE, 2004; Aulenta et al., 2005; Long and Borden, 2006).

4.4 Minimum design pH

While the initial solution pH affects the extent of dehalogenation likely to occur prior to reaching the inhibitory pH level, the minimum design pH controls the amount of bicarbonate amendment needed once this level is reached. As shown in Fig.

5, the bicarbonate requirement decreases significantly if microorganisms are able to tolerate more acidic conditions and the design pH can be lowered. With sulfate exhausted and assuming no gas release, the bicarbonate required to maintain pH = 6.2 is 3.1 mM per mM of dehalogenation compared with 7.2 mM per mM of dehalogenation for pH = 6.7. At low pH, the weak acids added from fermentation and the reduction of nonchlorinated electron acceptors (e.g., H_2S) dissociate less and therefore less acidity (H^+) is directly added to the solution per mM of dehalogenation. Furthermore, at lower pH each mole of bicarbonate added to the system has a greater neutralizing capacity (2). These points are further discussed in Section 5. The results also indicate that, due to the elevated concentrations of carbonate species associated with greater bicarbonate amendment, gas formation is more likely when more neutral conditions need to be maintained.

4.5 Use of acetate as electron donor (p)

Simulations were performed to determine the bicarbonate requirements when acetate is used as a direct electron donor for dehalogenation. The parameter *p* is used to specify the fraction of acetate produced from fermentation of the primary electron donor is used according to (4). The oxidation of acetate is beneficial because it not only reduces the total primary electron donor requirement, but as shown in Fig. 6 it also lowers the overall acidity generated and therefore bicarbonate requirement. In the absence of gas release, the total bicarbonate required if all of the acetate is used as an electron donor (p = 1) is 3.6 mM per mM of dehalogenation compared with 4.9 mM per mM of dehalogenation if acetate oxidization is inhibited (p = 0). Although two moles of CO_2 are produced per mol of acetate oxidized, the production of this weak acid is offset by the consumption of one mole of acetate. With linoelic acid used as the primary electron donor, each mole of acetate oxidized leads to a total reduction of acetate species of 3.57 mol per mol of dehalogenation. Although the carbonate produced directly from fermentation and dehalogenation is greater when acetate is oxidized, the simulations indicate that a gas phase forms more rapidly when acetate is not used. This is because the bicarbonate addition, and therefore the total carbonate species added to the system, is much greater for this case. These simulations suggest that if a conservative estimate is sought with regards to both the primary electron donor and bicarbonate requirements, it is better to assume that acetate is not used as an electron donor.

4.6 Influence of nonchlorinated TEAPs

Simulations were performed to investigate the influence of sulfate and iron(III) reduction on the acidity generated and bicarbonate requirements. Iron(III) and sulfate reducers are generally the dominant competitors for H_2 with dehalogenating microorganisms in DNAPL treatment zones. The individual influences of these TEAPs on the bicarbonate requirements are first examined and then their combined effects are discussed.

4.6.1 Sulfate reduction

The total bicarbonate requirement as the initial sulfate concentration varies is shown in Fig. 7a. To examine directly the effects of sulfate reduction on the acidity, no gas phase is allowed and there are no iron oxides present. For the same f_{min} (= 0.2), as the initial sulfate concentration reduces, sulfate is removed from the solution more rapidly. Once sulfate is removed, as there are no other nonchlorinated electron acceptors available, f switches from 0.2 to 1 and this is accompanied by a decrease in the bicarbonate required per mM of dehalogenation. This decrease in the bicarbonate required to maintain a constant pH indicates, perhaps surprisingly, that sulfate reduction may lead to a net addition of acidity. The reduction of one mole of sulfate generates 2 moles of alkalinity, however it also consumes 4 moles of H_2 (Table 2). With linoleic acid used as the electron donor, to supply 4 moles of H_2, 2.57 moles of acetic acid are produced. The generation of this acetic acid, if not oxidized, offsets the alkalinity benefits of sulfate reduction. The net effect of sulfate reduction, however, will vary significantly according to the specific electron donor used as each produces different by-products from fermentation.

In these simulations, the initial sulfate availability only influences the extent of dehalogenation before f switches to 1. With f_{min} = 0.2, for initial sulfate concentrations greater than 40 mM, sulfate is in excess and thus the model predicts the same total bicarbonate requirement for 40 mM of dehalogenation. Sulfate is likely to be in excess when sulfate-containing minerals such as gypsum or anhydrite are present, as these minerals are highly soluble and have rapid dissolution kinetics. This sensitivity analysis assumes that f_{min} is independent of sulfate concentration. In reality, the H_2 directed to sulfate reduction may increase as the sulfate concentration increases, and thus f_{min} will decrease. As f_{min} decreases the bicarbonate required per mM of dehalogenation increases due to the net acidity generated from sulfate reduction (Fig. 7b). However, the amount of H_2 diverted to sulfate reduction and thus the net acidity generated from this process is constrained by the initial amount of sulfate present. Therefore, for the same starting sulfate concentration, if all the sulfate is reduced the total bicarbonate requirement for 40 mM of dehalogenation is identical regardless of f_{min} (Fig. 7b, c.f. f_{min} = 0.2 and 0.5). As expected, with f_{min} = 1 the bicarbonate requirement is identical to the case when there is negligible sulfate present.

4.6.2 Iron(III) reduction

The influence of iron(III) reduction on the bicarbonate requirements is illustrated in Fig. 8. In these simulations there is negligible sulfate present and gas formation is not permitted. Although f_{min} is set at 0.2, f is adjusted based on the iron oxide dissolution and thus reduction rate. The results indicate that as the iron oxide reduction rate increases, the bicarbonate requirement decreases. Each mole of iron oxide reduced produces two moles of alkalinity, but only 0.5 moles of H_2 are consumed. For linoleic acid this H_2 demand equates to the production of 0.32 moles of acetic acid. Thus, in contrast with sulfate reduction, the reduction of iron oxide leads to a net addition of alkalinity, thus reducing the bicarbonate requirements. For the conditions simulated, the adjusted f ranges from 1 to 0.78 as k varies from 10^{-11} to $10^{-9.75}$ mol m^{-2} s^{-1}. The pH is predicted to remain above 6.5 for 40 mM of dehalogenation when k is greater than $10^{-9.5}$ mol m^{-2} s^{-1}.

The iron oxide reduction rate will likely increase as the mass fraction of iron oxides increases, in particular the fraction of freshly precipitated iron oxides such as ferrihydrite. Microbial catalysis however also plays an important role in the reduction of iron oxides with the process significantly enhanced when microbes are in direct contact with the iron oxide surface (Appelo and Postma, 2005). Although accurately predicting iron oxide reduction rates is difficult, our results show a consistent trend: increasing amounts of iron oxide reduction attenuate the amount of bicarbonate needed for pH control.

4.6.3 Sulfate and iron(III) reduction

Simulations were conducted to examine the influence of the H_2 efficiency with both sulfate and iron(III) available. The bicarbonate requirements for the base conditions with different f_{min} values adopted are shown in Fig. 9. The combined effects of sulfate and iron oxide reduction are complex because while sulfate reduction leads to a net addition of acidity, iron oxide reduction adds alkalinity. Furthermore when both sulfide and iron(II) are produced, iron sulfides precipitate leading to the addition of two moles of acidity (5). Based on the model setup, at each reaction step all of the iron(III) released into the solution (rate controlled, (6)) is reduced in preference to sulfate and therefore only the H_2 remaining after all the dissolved iron(III) is reduced is used for sulfate reduction.

The alkalinity generated directly from sulfate reduction is consumed if iron sulfides precipitate. Therefore, the net acidity added from sulfate reduction followed by iron sulfide precipitation is the 2.57 mol of acetic acid produced in the fermentation reaction to meet H_2 demand associated with sulfate reduction. As a result, the bicarbonate requirement is greatest when all the sulfate initially present is reduced and all of the sulfide produced precipitates (Fig. 9, f_{min} = 0.2). As f_{min} increases, only a fraction of the sulfate initially present is reduced and subsequently less iron sulfide precipitates (Fig. 9b,c). This is accompanied by a decrease in the total bicarbonate required. The bicarbonate requirements are lowest when the surplus H_2 produced from fermentation directly matches that required to reduce the iron(III) released into the solution at each reaction step and thus there is no H_2 left over for sulfate reduction (Fig. 9, f_{min} = 0.75). However as f_{min} approaches unity iron(III) reduction also decreases and as this process adds alkalinity, the bicarbonate requirement increases accordingly.

5. Simplified Model

Based on understanding gained from the PHREEQC model it is possible to develop a simplified set of equations that may be used for preliminary estimates of the amount of bicarbonate required once the minimum design pH is reached. At a given pH, the actual acidity added to the solution per mM of dehalogenation, and thus bicarbonate required to match this acidity, depends on the dissociation of the acids added from fermentation, dehalogenation and the nonchlorinated TEAPs. This dissociation varies according to pH. The initial solution alkalinity and pH influence the amount of dehalogenation that will occur prior to the minimum design pH being reached. Afterwards, however, these parameters do not influence the bicarbonate requirements and so they are not considered in the simplified model. The simulations also revealed that once bicarbonate addition commences, calcite's influence is not significant. Therefore, in developing a simplified model for the bicarbonate requirement, it is valid to neglect the potential dissolution and/or precipitation of calcite.

With linoleic acid used, each mole of dehalogenation adds 0.643 mol of acetic acid and one mol of HCl (Table 1). For the pH range 6 - 7 it can be assumed that these acids are completely dissociated and therefore 1.643 mol of H^+ are added per mol of dehalogenation. To neutralize this acidity it is necessary to add sufficient bicarbonate such that 1.643 mol of CO_2 will form, thus consuming the H^+ added to the solution (1). Based on the equilibrium expression describing the dissociation of CO_2 to HCO_3^- (2), the total bicarbonate needed to neutralize one mol of acidity is $1 + 10^{\mathrm{pH}-6.3}$. Therefore with linoleic acid used as the electron donor, the bicarbonate required to maintain a constant pH for one mol of dehalogenation ($R_{dehalogenation}$) is:

$$R_{dehalogenation} = 1.643\left(1 + 10^{\mathrm{pH}-6.3}\right). \tag{7}$$

The net acidity added to the solution and thus bicarbonate requirement associated with sulfate reduction can also be calculated. The dissociation constant for H_2S is $10^{-7.02}$ and so the reduction of one mol of sulfate produces $\frac{1}{10^{7.02-\mathrm{pH}}+1}$ mol of HS^- and $1-\frac{1}{10^{7.02-\mathrm{pH}}+1}$ mol of H_2S. S^{2-} is negligible at pH between 6 - 7. In consequence, sulfate reduction directly adds $2-\frac{1}{10^{7.02-\mathrm{pH}}+1}$ mol of alkalinity. However 4 mol of H_2 are consumed for each mol of sulfate reduced and with linoleic acid used as the electron donor, this is associated with the production of 2.57 mol of acetic acid and thus the addition of 2.57 mol of acidity. Thus, the bicarbonate required per mol of sulfate reduced ($R_{sulfate}$) is given by:

$$R_{sulfate}=\left(0.57+\frac{1}{10^{7.02-\mathrm{pH}}+1}\right)\left(1+10^{\mathrm{pH}-6.3}\right). \qquad (8)$$

In a similar manner it can be determined that with linoleic acid, the bicarbonate required per mol of iron oxide reduced (R_{iron}) is:

$$R_{iron}=-1.679\left(1+10^{\mathrm{pH}-6.3}\right). \qquad (9)$$

This equation illustrates, as previously shown in Section 4.6.2, that iron(III) reduction may decrease the bicarbonate requirement. Finally, iron sulfide precipitation removes the H_2S and HS^- produced from sulfate reduction and thus the acidity added when this precipitate forms is identical to the alkalinity added directly from sulfate reduction. Therefore, the bicarbonate required per mol of iron sulfide that precipitates (R_{FeS}) is:

$$R_{FeS}=\left(2-\frac{1}{10^{7.02-\mathrm{pH}}+1}\right)\left(1+10^{\mathrm{pH}-6.3}\right). \qquad (10)$$

For a given amount of sulfate and iron(III) reduction, and iron sulfide precipitation per mol of dehalogenation, (7) to (10) can be used to estimate the overall bicarbonate requirement (= $R_{dehalogenation} + R_{sulfate} + R_{iron} + R_{FeS}$). As (7) to (10) are based on the dissociation of acids at a constant pH, they are only applicable once the minimum design pH is reached. They do not allow prediction of the extent of dehalogenation likely to occur prior to this pH being reached. Potential gas bubble formation and use of acetate as an electron donor (p = 0) are neglected also, the implications of which are discussed below.

We now use this simplified model to estimate the bicarbonate requirements for the base conditions and compare the results to the PHREEQC geochemical model predictions (Section 4.1). The amount of iron(III) and sulfate reduction, and iron sulfide precipitating per mol of dehalogenation must first be estimated. Assuming the surface area of iron oxide is constant, from (6) the rate of iron oxide reduction at a pH = 6.5 with $k = 10^{-10.2}$ can be approximated as 0.106 mM d^{-1}. For the base conditions the dehalogenation rate is 0.4 mM d^{-1} (40 mM of dehalogenation occurs over 100 d). By comparing these time scales it can be determined that 0.265 mM of iron(III) will be reduced per mM of dehalogenation. With the same f_{min} (= 0.2), 4 mM H_2 per mM of dehalogenation are available for the reduction of nonchlorinated electron acceptors. With 0.265 mM of iron(III) reduced, 3.87 mM of H_2 are available for sulfate reduction and this equates to the reduction of 0.976 mM of sulfate per mM of dehalogenation. The precipitation of iron sulfides is limited by the iron(II) availability and therefore 0.265 mM of iron sulfide will form per mM of dehalogenation. Thus, for the base conditions with sulfate available, using (7) to (10) and with a pH = 6.5, the bicarbonate required per mM of dehalogenation is estimated at 6.3 mM. When the sulfate is removed the amount of iron(III) reduced per mM of dehalogenation will remain at

0.265 mM. For 40 mM of dehalogenation and this rate of iron(III) reduction, there will be sufficient sulfide available in solution, even once sulfate is exhausted, for iron sulfide to continue to precipitate as iron(II) is produced (i.e., 0.265 mM of iron sulfide precipitate per mM of dehalogenation). In applying (7), (9) and (10) the bicarbonate required is estimated at 4.3 mM per mM of dehalogenation. In comparing these estimates with the PHREEQC model predictions (Table 5), it can be seen that the simplified model under predicts the bicarbonate requirements. As potential gas release and acetate oxidization are also neglected in the PHREEQC simulations used for this comparison, the underestimation is primarily due to the extensive speciation processes included in the PHREEQC model (e.g., formation of aqueous species such as $NaHCO_3$ and $KHCO_3$).

Equations (7) - (10) assume that linoleic acid is used as the electron donor, however similar equations have been developed (Table 6) for all common electron donors listed in Table 1. For lactic acid, glucose and methanol the CO_2 produced from fermentation is included in the simplified model as this increases the bicarbonate requirement. In a similar manner, the HCO_3^- produced upon fermentation of sodium lactate is also considered. A comparison of the bicarbonate requirements predicted using the geochemical model and using these equations for each electron donor is shown in Table 5 for the two different f values. For all donors considered, the comparison is reasonable with the simplified approach generally under predicting the bicarbonate requirement relative to the PHREEQC model, typically by between 15 and 20%. The difference in the estimates increases as the bicarbonate requirement decreases (i.e., methanol for f_{min} = 0.2). This is because the aqueous speciation processes included in PHREEQC have a greater relative impact as the bicarbonate requirement decreases. The simplified model does not include the use of acetate as an electron donor or the release of CO_2. As these processes both reduce the bicarbonate requirements (e.g., see Fig. 3b and Fig. 6, respectively) and will likely occur, the lower simplified model estimates may actually be more in line with field conditions. Therefore, for a preliminary design estimate, the expressions in Table 6 provide a simple means to estimate the field bicarbonate requirements. The simplified model also provides important quantitative understanding of the processes influencing the amount of acidity generated (e.g., electron donor selection). For more detailed design however, the more detailed modeling approach might be considered.

6. Conclusions

This study provides insight into the acidity generated and the bicarbonate addition required to maintain the pH in the DNAPL source zone within the optimal range for dehalogenating bacteria. The major findings are outlined below.

- Where extensive dehalogenation is likely to occur in the DNAPL source zone, significant bicarbonate addition may be necessary even in soils that are naturally well-buffered. While calcite provides some pH control, its buffering capacity is limited by solubility constraints and may not be sufficient to prevent acidic conditions developing.
- The choice of electron donor strongly influences the bicarbonate requirements due to the relative amounts of acetate, carbonate species and sodium associated with the fermentation process (Table 1).
- The bicarbonate required per mM of dehalogenation depends not only on the electron donor fermentation and dehalogenation processes but also on the competing nonchlorinated TEAPs. Although sulfate and iron oxide reduction both add alkalinity to the solution (Table 2), these alkalinity benefits can be

counterbalanced by the acidity (e.g., acetic acid) added in producing the H_2 consumed by these TEAPs. Whether sulfate and iron(III) reduction lead to a net generation of alkalinity depends on the specific electron donor used (Table 6). If both iron(III) and sulfate reduction occur, iron sulfides are likely to precipitate and this adds acidity to the solution, thus increasing the bicarbonate requirement.

- The formation of a gas phase and thus the release of CO_2 lowers the bicarbonate required per mM of dehalogenation due to the shift in the dissolved carbonate equilibria (2).
- The bicarbonate requirement depends strongly on the minimum design pH with the requirement increasing significantly with increase in design pH towards the more neutral value more favored by dehalogenating bacteria.

Acknowledgements

The authors acknowledge the advice provided by Mark Harkness, Mike Lee, James Dyer, David Ellis and other members of project SABRE (Source Area BioREmediation, www.claire.co.uk/sabre). Support from BBSRC BB/B519076/1 and SNF 200021_120160 is acknowledged.

References

Adamson DA, Lyon DY, Hughes JB. Flux and product distribution during biological treatment of tetrachloroethene dense non-aqueous-phase liquid. Environmental Science and Technology 2004;38:2021-2028.

AFCEE. Principles and Practices of Enhanced Anaerobic Bioremediation of Chlorinated Solvents. US Department of Defense, Air Force Center for Environmental Excellence and the Environmental Security Technology Certification Program (ESTCP). Washington, DC, 2004.

Amos B, Christ J, Abriola L, Pennell KD, Loffler FE. Experimental evaluation and mathematical modeling of microbially enhanced tetrachloroethene (PCE) dissolution. Environmental Science and Technology 2007;41:963-970.

Amos BK, Suchomel EJ, Pennell KD, Loffler FE. Microbial activity and distribution during enhanced contaminant dissolution from a NAPL source zone. Water Research 2008;42:2963-2974.

Amos RT, Mayer KU. Investigating the role of gas bubble formation and entrapment in contaminated aquifers: Reactive transport modelling. Journal of Contaminant Hydrology 2006;87:123-154.

Appelo CAJ, Postma D. Geochemistry, Groundwater and Pollution. A. A. Balkema Publishers, Amsterdam, 2005, 2^{nd} ed.

Aulenta F, Gossett JM, Papini MP, Rossetti S, Majone M. Comparative study of methanol, butyrate, and hydrogen as electron donors for long-term dechlorination of tetrachloroethene in mixed anaerobic cultures. Biotechnology and Bioengineering 2005;91:743-753.

Aulenta F, Majone M, Tandoi V. Enhanced anaerobic bioremediation of chlorinated solvents: Environmental factors influencing microbial activity and their relevance under field conditions. Journal of Chemical Technology and Biotechnology 2006;81:1463-1474.

Aulenta F, Pera A, Rossetti S, Papini MP, Majone M. Relevance of side reactions in anaerobic reductive dechlorination microcosms amended with different electron donors. Water Research 2007;41:27-38.

Carr CS, Hughes JB. Enrichment of high-rate PCE dechlorination and comparative study of lactate, methanol, and hydrogen as electron donors to sustain activity. Environmental Science and Technology 1998;32:1817-1824.

Christ JA, Ramsburg CA, Abriola LM, Pennell KD, Loffler FE. Coupling aggressive mass removal with microbial reductive dechlorination for remediation of DNAPL source zones: A review and assessment. Environmental Health Perspectives 2005;113:465-477.

Chu M, Kitanidis PK, McCarty PL. Possible factors controlling the effectiveness of bioenhanced dissolution of non-aqueous phase tetrachloroethene. Advances in Water Resources 2004;27:601-615.

Cirpka OA, Windfuhr C, Bisch G, Granzow S, Scholz-Muramatsu H, Kobus H. Microbial reductive dechlorination in large-scale sandbox model. Journal of Environmental Engineering-ASCE 1999;125:861-870.

Cope N, Hughes JB. Biologically-enhanced removal of PCE from NAPL source zones. Environmental Science and Technology 2001;35:2014-2021.

Curtis GP. Comparison of approaches for simulating reactive solute transport involving organic degradation reactions by multiple terminal electron acceptors. Computers and Geosciences 2003;29:319-329.

Da Silva ML, Daprato RC, Gomez DE, Hughes JB, Ward CH, Alvarez PJ. Comparison of bioaugmentation and biostimulation for the enhancement of dense nonaqueous phase liquid source zone bioremediation. Water Environment Research 2006;78:2456-2465.

Dolfing J, Janssen DB. Estimates of Gibbes free energies of formation of chlorinated aliphatic compounds. Biodegradation 1994;5:21-28.

Dolfing J, Tiedje JM. Acetate as a source of reducing equivalents in the reductive dechlorination of 2,5-dichlorobenzoate. Archives of Microbiology 1991;156:356-361.

Ellis DE, Lutz EJ, Odom JM, Buchanan RJ, Bartlett CL, Lee MD, Harkness MR, Deweerd KA. Bioaugmentation for accelerated in situ anaerobic bioremediation. Environmental Science and Technology 2000;34:2254-2260.

Fennell DE, Gossett JM, Zinder SH. Comparison of butyric acid, ethanol, lactic acid, and propionic acid as hydrogen donors for the reductive dechlorination of tetrachloroethene. Environmental Science and Technology 1997;31:918-926.

He J, Sung Y, Dollhope ME, Fathepure BZ, Tiedje JM, Loffler FE. Acetate versus hydrogen as direct electron honors to stimulate the microbial reductive dechlorination process at chloroethene-contaminated sites. Environmental Science and Technology 2002;36:3945-3952.

Heimann AC, Friis AK, Jakobsen R. Effects of sulfate on anaerobic chloroethene degradation by an enriched culture under transient and steady-state hydrogen supply. Water Research 2005;39:3579-3586.

Hoelen TP, Reinhard M. Complete biological dehalogenation of chlorinated ethylenes in sulfate containing groundwater. Biodegradation 2004;15:395-403.

Jakobsen R, Postma D. Redox zoning, rates of sulphate reduction and interactions with Fe-reduction and methanogenesis in a shallow sandy aquifer, Romo, Denmark. Geochimica et Cosmochimica Acta 1999;63:137-151.

Krumholz LR, Sharp R, Fishbain SS. A freshwater anaerobe coupling acetate oxidation to tetrachloroethylene dehalogenation. Applied and Environmental Microbiology 1996;62:4108-4113.

Lee IS, Bae JH, McCarty PL. Comparison between acetate and hydrogen as electron donors and implications for the reductive dehalogenation of PCE and TCE. Journal of Contaminant Hydrology 2007; 94:76-85.

Loffler FE, Edwards EA. Harnessing microbial activities for environmental cleanup. Current Opinion in Biotechnology 2006;17:274–284.

Loffler FE, Sun Q, Li J, Tiedje JM. 16S rRNA gene-based detection of tetrachloroethene-dechlorinating Desulfuromonas and Dehalococcoides species. Applied and Environmental Microbiology 2000;66:1369-1374.

Loffler FE, Tiedje JM, Sanford RA. Fraction of electrons consumed in electron acceptor reduction and hydrogen thresholds as indicators of halorespiratory physiology. Applied and Environmental Microbiology 1999;65:4049-4056.

Long CM, Borden RC. Enhanced reductive dechlorination in columns treated with edible oil emulsion. Journal of Contaminant Hydrology 2006; 87 54-72.

Major DW, McMaster ML, Cox EE, Edwards EA, Dworatzek SM, Hendrickson ER, Starr MG, Payne JA, Buonamici LW. Field demonstration of successful bioaugmentation to achieve dechlorination of tetrachloroethene to ethene. Environmental Science and Technology 2002;36:5106-5116

Maurer M, Rittmann BE. Modeling intrinsic bioremediation for interpret observable biogeochemical footprints of BTEX biodegradation: The need for fermentation and abiotic chemical processes. Biodegradation 2004;15:405-417.

McCarty PL. Breathing with chlorinated solvents. Science 1997;276.:1521-1522.

McCarty PL, Chu MY, Kitanidis PK. Electron donor and pH relationships for biologically enhanced dissolution of chlorinated solvent DNAPL in groundwater. European Journal of Soil Science 2007;43:276-282.

Middeldorp PJM, Luijten MLGC, van de Pas BA, van Eekert MHA, Kengen SWM, Schraa G, Stams AJM. Anaerobic microbial reductive dehalogenation of chlorinated ethenes. Bioremediation Journal 1999;3:151-169.

National Research Council. Contaminants in the subsurface: source zone assessment and remediation. Washington, DC., 2004.

Neumann A, Scholz-Muramatsu, H., Diekert, G.,. Tetrachloroethene metabolism of Dehalospirillum multivorans. Archives of Microbiology 1994;162:295–301.

Parkhurst DL, Appelo CAJ. User's guide to PHREEQC (Version 2) – A computer program for speciation, batch-reaction, one-dimensional transport, and inverse geochemical calculations, Water-Resources Investigations Report 99-4259. US Geological Survey. Denver, CO, 1999.

Payne FC, Suthersan SS, Nelson DK, Suarez G, Tasker I, Akladiss N. Enhanced reductive dechlorination of PCE in unconsolidated soils. Remediation 2006;17:5-21.

Rickard D. Kinetics of FeS precipitation: Part 1. Competing reaction mechanism. Geochimica et Cosmochimica 1995;59:4367-4379.

Rivett M, Shepherd K, Keeys L, Brennan A. Chlorinated solvents in the Birmingham aquifer, UK: 1986-2001. Quarterly Journal of Engineering Geology and Hydrogeology 2005;38:337-350.

Roden EE. Geochemical and microbiological controls on dissimilatory iron reduction. Comptes Rendus Geoscience 2006;338:456-467.

Schumacher W, Holliger C. The proton/electron ration of the menaquinone-dependent electron transport from dihydrogen to tetrachloroethene in "Dehalobacter restrictus". Journal of Bacteriology 1996;178:2328-2333.

Sharma PK, McCarty PL. Isolation and characterization of a facultatively aerobic bacterium that reductively dehalogenates tetrachloroethene to cis-1,2-dichloroethene. Applied and Environmental Microbiology 1996;62:761-765.

Singh H, Bajwa MS. Comparison of different models for describing gypsum dissolution kinetics in different aqueous salt solutions. Australian Journal of Soil Research 1990;28:947-953.

Sung Y, Ritalahti KM, Sanford RA, Urbance JW. Characterization of two tetrachloroethene-reducing, acetate-oxidizing anaerobic bacteria and their description as Desulfuromonas michiganensis sp. nov. Applied and Environmental Microbiology 2003;69:2964-2974.

Yang Y, McCarty PL. Biologically enhanced dissolution of tetrachloroethene DNAPL. Environmental Science and Technology 2000;34:2979-2989.

Yang Y, McCarty PL. Comparison between donor substrates for biologically enhanced tetrachloroethene DNAPL dissolution. Environmental Science and Technology 2002;36:3400-3404.

Table 1. Fermentation reactions for common electron donors and amounts of carbonate species ($\Sigma[CO_2 + HCO_3^-]$), acetate species ($\Sigma[CH_3COOH + CH_3COO^-]$) and sodium ($Na^+$) added per mol of H_2 produced. The total moles of by-products added per mol of dehalogenation can be calculated by multiplying the amounts provided by 1/*f*.

Electron donor	Fermentation reaction	Overall reaction for dehalogenation and fermentation	$\Sigma(CO_2 + HCO_3^-)$	$\Sigma(CH_3COOH + CH_3COO^-)$	Na^+
Linoleic acid	$C_{18}H_{32}O_2 + 16H_2O = 14H_2 + 9CH_3COOH$	$R\text{-}Cl + \frac{1}{14f} C_{18}H_{32}O_2 + \frac{8}{7f} H_2O = R\text{-}H + HCl + \frac{9}{14f} CH_3COOH + \frac{(1-f)}{f} H_2$	0	0.643	0
Sodium Lactate	$CH_3CHOHCOONa + 2H_2O = 2H_2 + CH_3COOH + NaHCO_3$	$R\text{-}Cl + \frac{1}{2f} CH_3CHOHCOONa + \frac{1}{f} H_2O = R\text{-}H + HCl + \frac{1}{2f} CH_3COOH + \frac{1}{2f} NaHCO_3 + \frac{(1-f)}{f} H_2$	0.5	0.5	0.5
Lactic acid	$CH_3CHOHCOOH + H_2O = 2H_2 + CH_3COOH + CO_2$	$R\text{-}Cl + \frac{1}{2f} CH_3CHOHCOOH + \frac{1}{2f} H_2O = R\text{-}H + HCl + \frac{1}{2f} CH_3COOH + \frac{1}{2f} CO_2 + \frac{(1-f)}{f} H_2$	0.5	0.5	0
Glucose	$C_6H_{12}O_6 + 2H_2O = 4H_2 + 2CH_3COOH + 2CO_2$	$R\text{-}Cl + \frac{1}{4f} C_6H_{12}O_6 + \frac{1}{2f} H_2O = R\text{-}H + HCl + \frac{1}{2f} CH_3COOH + \frac{1}{2f} CO_2 + \frac{(1-f)}{f} H_2$	0.5	0.5	0
Butyric acid	$CH_3CH_2CH_2COOH + 2H_2O = 2H_2 + 2CH_3COOH$	$R\text{-}Cl + \frac{1}{2f} CH_3CH_2CH_2COOH + \frac{1}{f} H_2O = R\text{-}H + HCl + \frac{1}{f} CH_3COOH + \frac{(1-f)}{f} H_2$	0	1	0

Methanol	$CH_3OH + H_2O = 3H_2 + CO_2$	$R\text{-}Cl + \frac{1}{f}CH_3OH + \frac{1}{3f}H_2O = R\text{-}H + HCl + \frac{1}{3f}CO_2 + \frac{(1-f)}{f}H_2$	0.33	0	0
Ethanol	$CH_3CH_2OH + H_2O = 2H_2 + CH_3COOH$	$R\text{-}Cl + \frac{1}{2f}CH_3CH_2OH + \frac{1}{2f}H_2O = R\text{-}H + HCl + \frac{1}{2f}CH_3COOH + \frac{(1-f)}{f}H_2$	0	0.5	0
Formate	$HCOONa + H_2O = NaHCO_3 + H_2$	$R\text{-}Cl + \frac{3}{14f}HCOONa + \frac{1}{f}H_2O = R\text{-}H + HCl + \frac{1}{f}NaHCO_3 + \frac{(1-f)}{f}H_2$	1	0	1

Table 2. Terminal electron-accepting processes (TEAPs) and amounts of alkalinity (OH^-) produced and H_2 consumed per mol of electron acceptor reduced.

	Reaction	Alkalinity added (per mol)	H_2 consumed (per mol)
Oxygen reduction	$O_2 + 2H_2 = 2H_2O$	0	2
Nitrate reduction	$2NO_3^- + 5H_2 = N_2 + 2OH^- + 4H_2O$	1	2.5
Iron oxide reduction			
Goethite	$2FeOOH(s) + H_2 = 2Fe^{2+} + 4OH^-$	2	0.5
Ferrihydrite	$2Fe(OH)_3(s) + H_2 = 2Fe^{2+} + 4OH^- + 2H_2O$	2	0.5
Dehalogenation	$R\text{-}Cl + H_2 = R\text{-}H + H^+ + Cl^-$	-1	1
Sulfate reduction	$SO_4^{2-} + 4H_2 = H_2S + 2OH^- + 2H_2O$	2	4
Methanogenesis	$CO_2 + 4H_2 = CH_4 + 2H_2O$	0	4

Table 3. Initial groundwater composition for base case.

Constituent	Concentration
pH	7
Alkalinity	220 mg L^{-1} $CaCO_3$
Ca^{2+}	8.1 mM
Cl^-	9.0 mM
K^+	2.0 mM
Mg^{2+}	5.0 mM
Na^+	6.0 mM
SO_4^{2-}	10.4 mM
N_2	Partial pressure = 0.79

Table 4. Amounts of mineral dissolved for 40 mM of dehalogenation. The initial moles of mineral present per kg of water are typical and are based on the mineralogy at a contaminated chlorinated solvent site currently undergoing enhanced bioremediation as part of the SABRE project.

Mineral	Initial amount present (mol kg of water^{-1})	Amount dissolved (mol kg of water^{-1})
Calcite	0.5	3.87×10^{-2}
Gypsum	0.1	1.83×10^{-2}
Goethite	3.3	1.71×10^{-2}
Anorthite	0.5	4.02×10^{-4}
Albite	0.16	1.55×10^{-5}
K-Feldspar	0.43	1.33×10^{-5}
Illite	0.41	1.27×10^{-5}
Chlorite	0.04	1.26×10^{-5}

Table 5. Predicted extent of dehalogenation that occurs while lowering the pH from the initial value of 7 to the design value of 6.5, and the bicarbonate required per mM of dehalogenation to maintain pH = 6.5 as calculated using the PHREEQC model, and the simplified model (Section 5). Results are for the base case discussed in Section 4.1.

	PHREEQC model			Simplified model (Section 5)	
	Dehalogenation before pH < 6.5 (mM)	Bicarbonate required for *f* = 0.2 (mM)	Bicarbonate required for *f* = 0.88 (mM)	Bicarbonate required for *f* = 0.2 (mM)	Bicarbonate required for *f* = 0.88 (mM)
Linoleic acid	4.5	7.5	4.9	6.3	4.3
Sodium lactate	5	3.3	4.0	2.0	3.3
Lactic acid/Glucose	2.2	10	5.8	8.8	5.1
Butyric acid	2.7	12.8	6.4	11.0	5.4
Methanol	7.6	2.6	3.5	0.6	3.0
Ethanol	6.5	5.8	4.5	4.5	3. 9
Formate	pH = 6.6 after 40 mM of dehalogenation				

Table 6. Simplified model to calculate the net acidity added per mol of dehalogenation, sulfate reduction, iron oxide reduction and iron sulfide precipitation for common electron donors at the minimum design pH. The acidity generated is multiplied by $1+10^{\text{pH}-6.3}$ to calculate the total bicarbonate required per mol of dehalogenation. These equations neglect potential gas release and acetate oxidization.

	Dehalogenation	Sulfate reduction	Iron oxide reduction	Iron sulfide precipitation
Linoleic acid	1.643	$0.57+\frac{1}{10^{7.02-\text{pH}}+1}$	-1.679	$2-\frac{1}{10^{7.02-\text{pH}}+1}$
Lactic acid/Glucose	$1.5+0.5\frac{10^{\text{pH}-6.3}}{10^{\text{pH}-6.3}+1}$	$2\frac{10^{\text{pH}-6.3}}{10^{\text{pH}-6.3}+1}+\frac{1}{10^{7.02-\text{pH}}+1}$	$0.25\frac{10^{\text{pH}-6.3}}{10^{\text{pH}-6.3}+1}-1.75$	$2-\frac{1}{10^{7.02-\text{pH}}+1}$
Sodium lactate	$1.5-\frac{0.5}{10^{\text{pH}-6.3}+1}$	$-\frac{2}{10^{\text{pH}-6.3}+1}+\frac{1}{10^{7.02-\text{pH}}+1}$	$-\frac{0.25}{10^{\text{pH}-6.3}+1}-1.75$	$2-\frac{1}{10^{7.02-\text{pH}}+1}$
Butyric acid	2	$2+\frac{1}{10^{7.02-\text{pH}}+1}$	-1.5	$2-\frac{1}{10^{7.02-\text{pH}}+1}$
Methanol	$1+0.33\frac{10^{\text{pH}-6.3}}{10^{\text{pH}-6.3}+1}$	$1.33\frac{10^{\text{pH}-6.3}}{10^{\text{pH}-6.3}+1}+\frac{1}{10^{7.02-\text{pH}}+1}-2$	$0.167\frac{10^{\text{pH}-6.3}}{10^{\text{pH}-6.3}+1}-2$	$2-\frac{1}{10^{7.02-\text{pH}}+1}$
Ethanol	1.5	$\frac{1}{10^{7.02-\text{pH}}+1}$	-1.75	$2-\frac{1}{10^{7.02-\text{pH}}+1}$

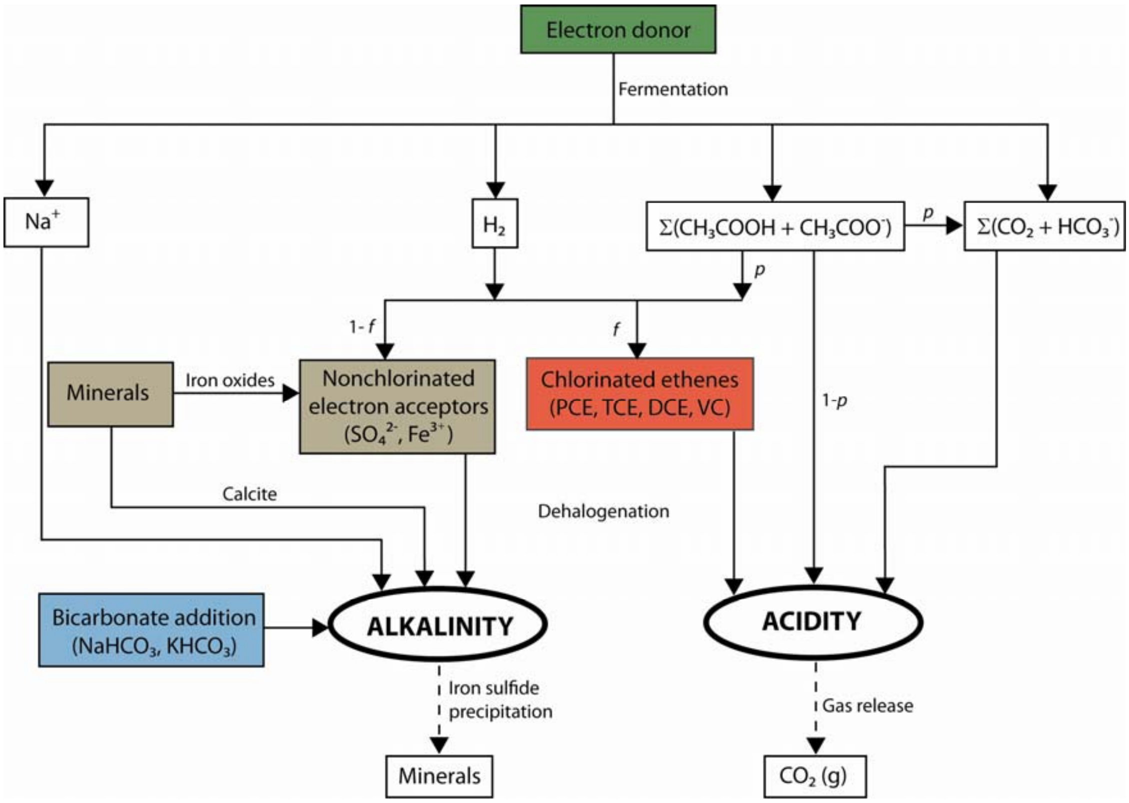

Figure 1. Main factors influencing the solution acidity and alkalinity. To maintain a constant pH the acidity and alkalinity additions (including bicarbonate addition) must balance. A description of the processes is provided in Section 2.

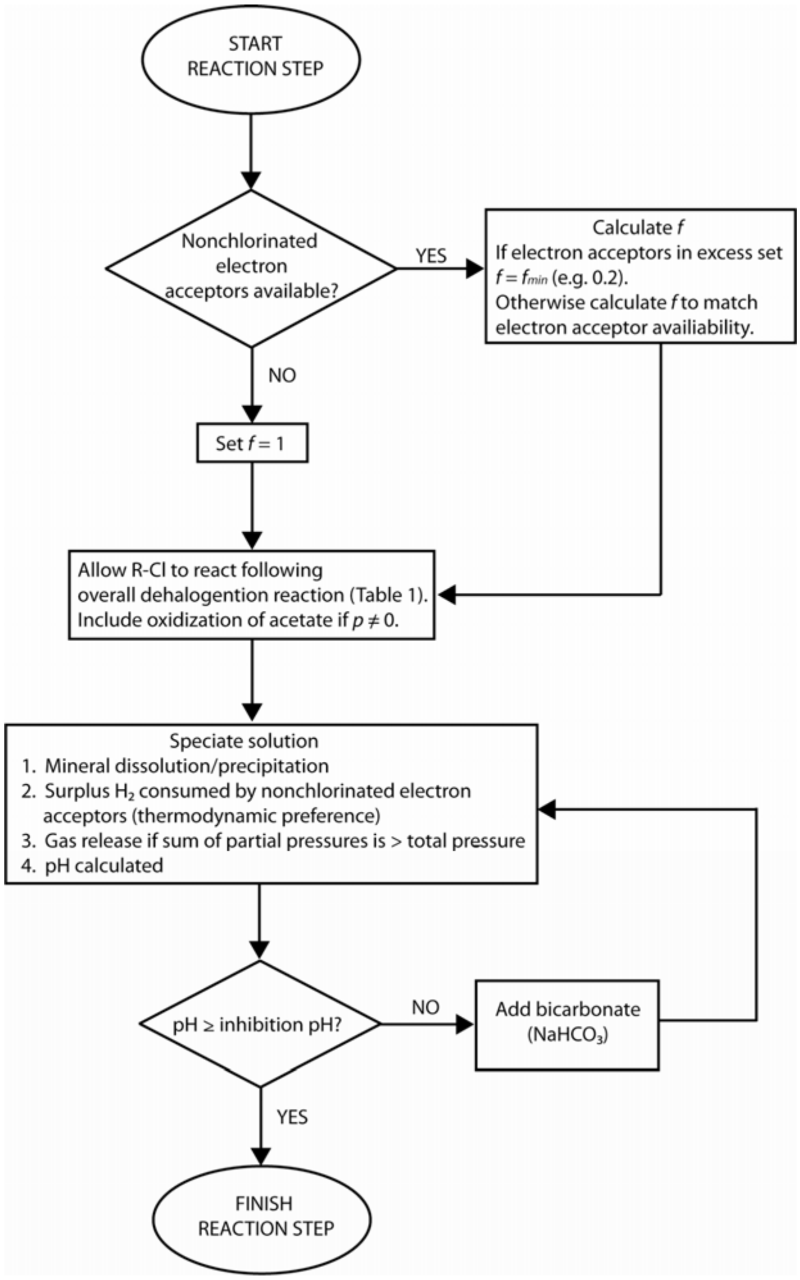

Figure 2. Flow chart of model algorithm for each reaction step. For the simulations presented, the dehalogenation of 40 mM of chlorinated ethene equivalents occurs over 500 reaction steps and therefore at each step 40/500 mM of R-Cl is allowed to react according to the overall dehalogenation and fermentation reaction (Table 1). A description of the algorithm is provided in Section 2.

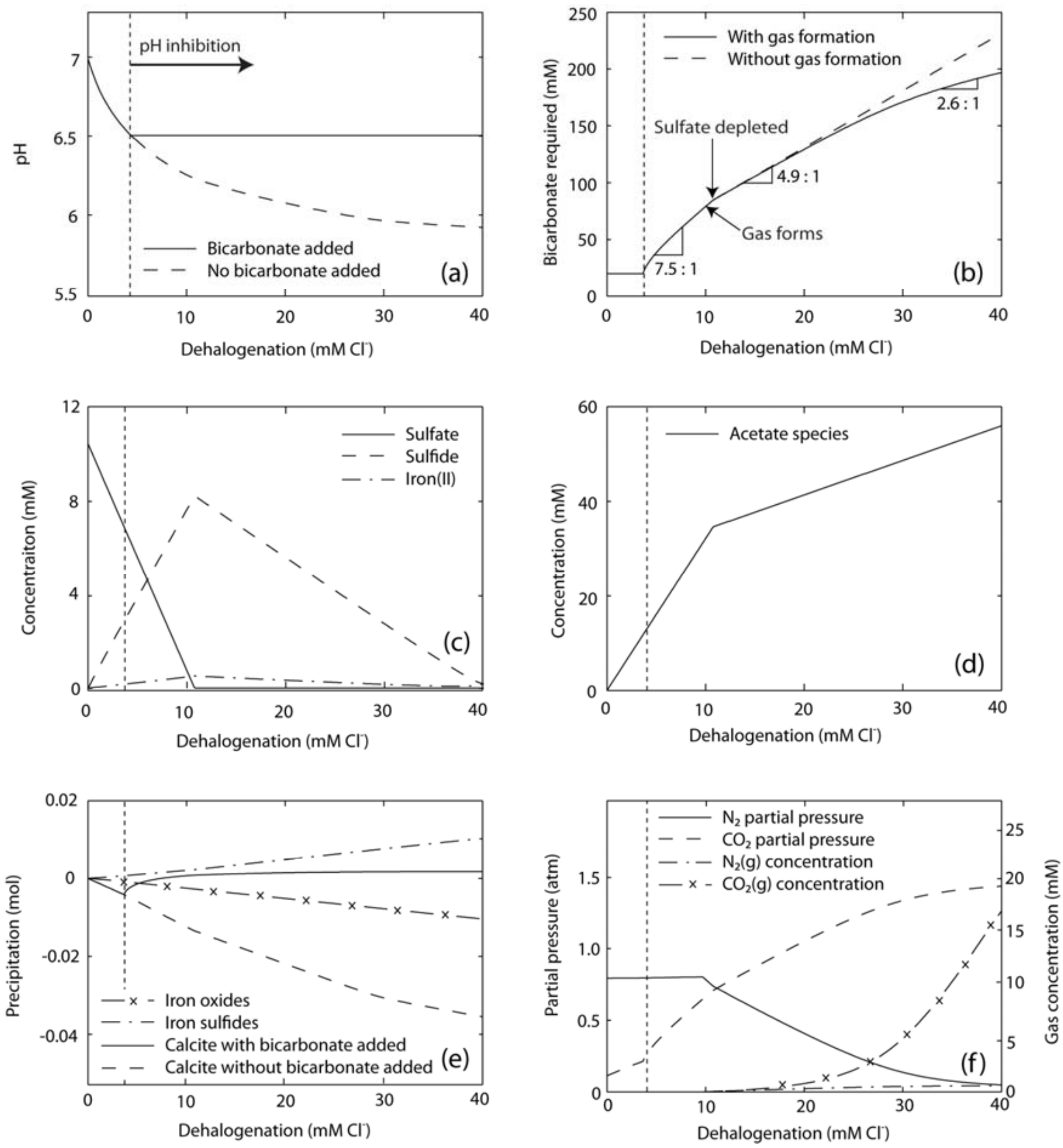

Figure 3. Effect of the extent of dehalogenation for the base conditions with linoleic acid used as the electron donor on (a) pH with and without bicarbonate addition, (b) bicarbonate required to maintain pH at or above 6.5, (c) concentrations of sulfate, sulfide and iron(II) with bicarbonate addition, (d) concentration of acetate species with bicarbonate addition, (e) change in calcite without bicarbonate addition and change in calcite, iron oxides and iron sulfides with bicarbonate addition, and (f) partial pressures of N_2 and

CO_2 and concentrations of N_2(g) and CO_2(g) with bicarbonate addition. The ratios listed below the curve in (b) give the amount of bicarbonate (mM) required per mM of dehalogenation (Section 4.1). Note that in (e) negative precipitation implies dissolution. Vertical dashes in each plot indicate the point at which pH control is necessary.

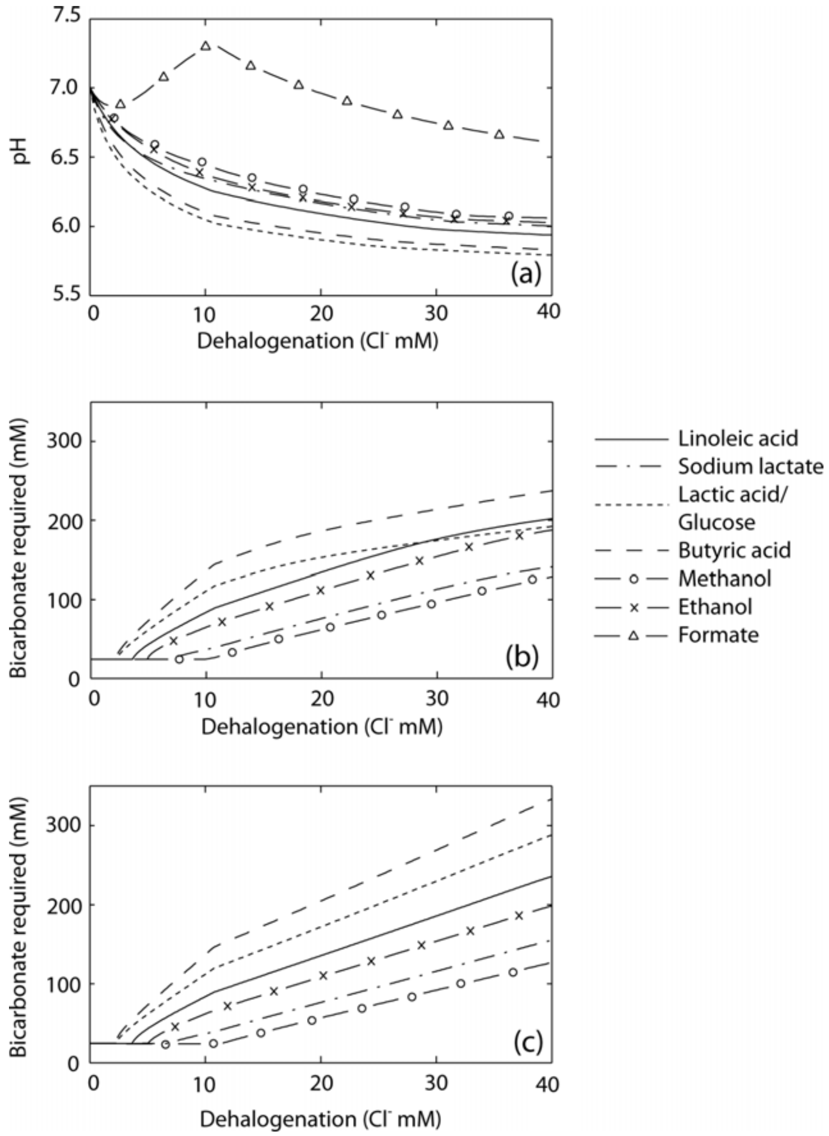

Figure 4. Effect of different electron donors on the (a) pH without bicarbonate addition, (b) bicarbonate required to maintain pH at or above 6.5 with gas release, and (c) bicarbonate required to maintain pH at or above 6.5 without gas release. Note that the amount of bicarbonate required when formate is used is zero and therefore formate is not plotted in (b) and (c).

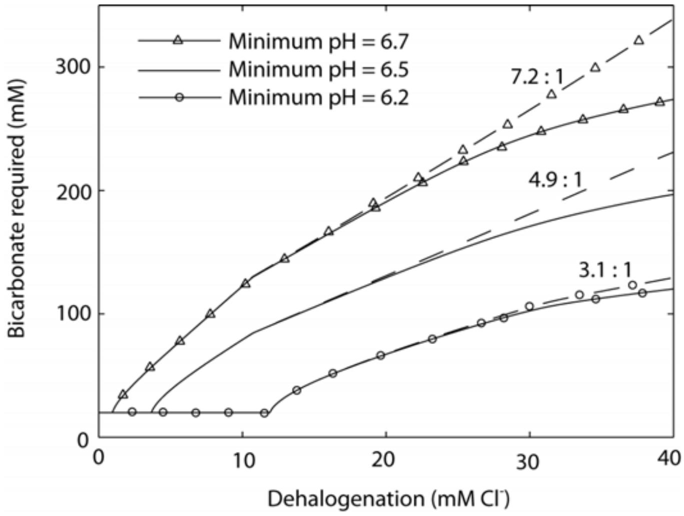

Figure 5. Bicarbonate required as dehalogenation proceeds for different minimum design pH values. Results are for the base conditions in which linoleic acid is the electron donor. For each minimum pH the bicarbonate required when no gas is allowed to form are also shown (dashed lines). The amounts of bicarbonate required per mM of dehalogenation when there is no gas release and $f = 0.88$ are listed above the curves.

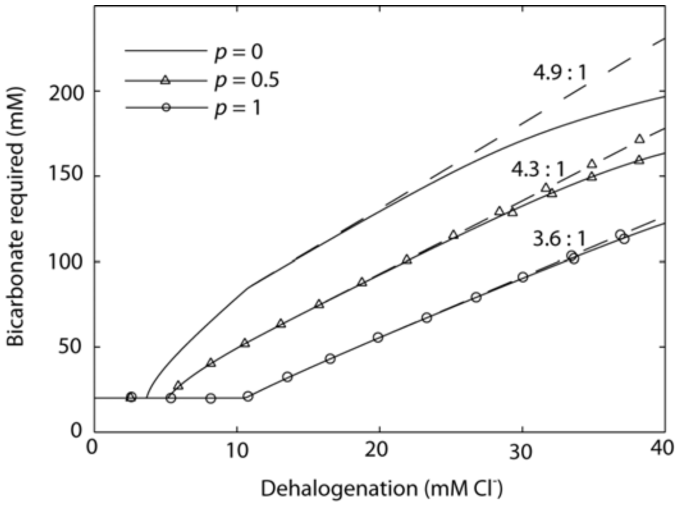

Figure 6. Bicarbonate required to maintain the pH at or above 6.5 with p = 0 (no acetate oxidation), p = 0.5 and p = 1 (complete oxidation of acetate) as dehalogenation proceeds. Results are for the base conditions in which linoleic acid is the electron donor. For each value of p, the amount of bicarbonate required when no gas is allowed to form is also shown (dashed lines). The amounts of bicarbonate required per mM of dehalogenation when there is no gas release and f = 0.88 are listed above the curves.

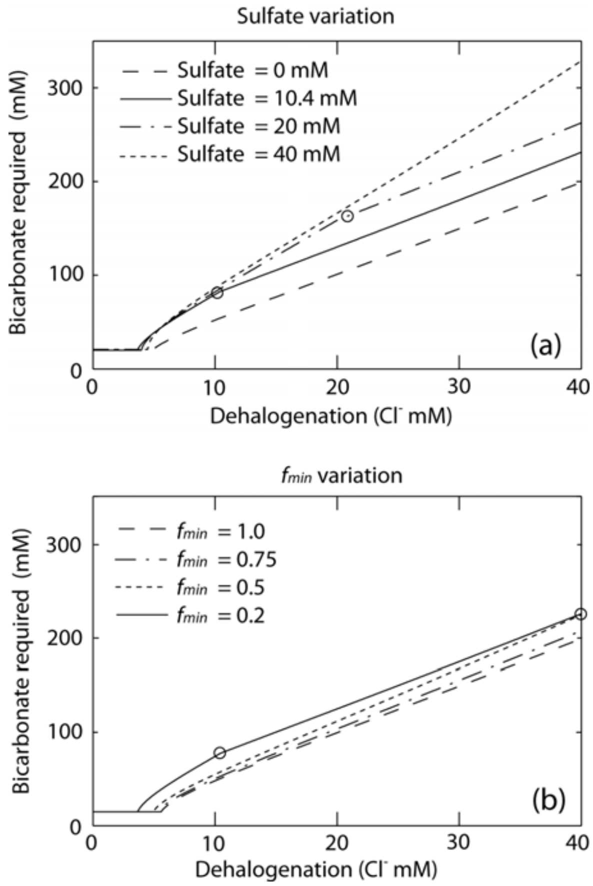

Figure 7. Influence of (a) initial sulfate concentration and (b) minimum H_2 efficiency (f_{min}) on the bicarbonate required to maintain the pH at or above 6.5 with sulfate reduction the sole nonchlorinated TEAP. Other than the variation of these parameters and absence of iron oxides and gas formation, the results are for the base conditions in which linoleic acid is the electron donor and sulfate is present initially at 10.4 mM. The open circles (○) show the points where sulfate is exhausted and *f* switches to 1.

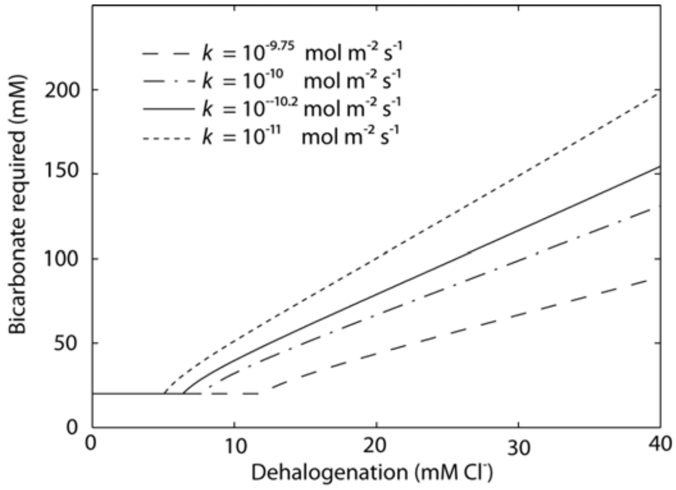

Figure 8. Influence of iron oxide dissolution and reduction rate constant (*k*) on bicarbonate required to maintain the pH at or above 6.5 with iron(III) reduction the sole nonchlorinated TEAP. Other than the variation of *k* and absence of sulfate and gas formation, the results are for the base conditions in which linoleic acid is the electron donor.

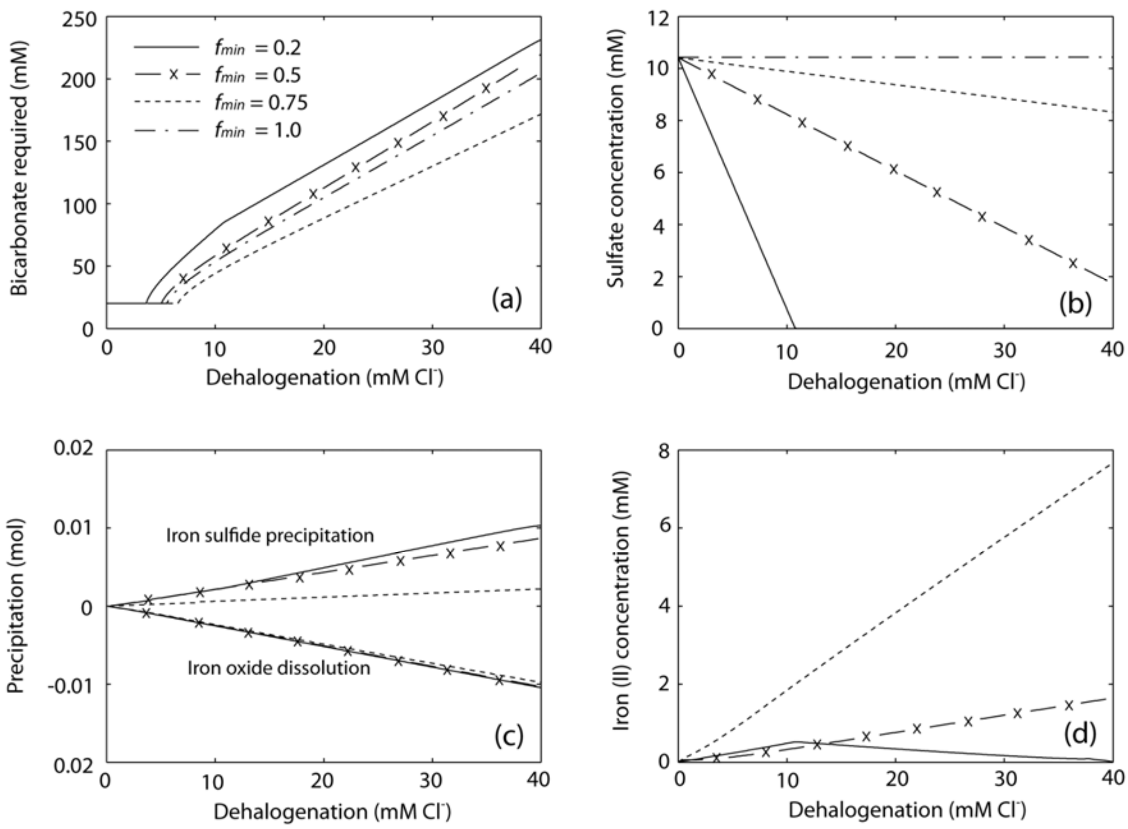

Figure 9. Influence of minimum H_2 efficiency (f_{min}) on (a) bicarbonate required to maintain the pH at or above 6.5, (b) sulfate concentration, (c) iron oxide dissolution and iron sulfide precipitation, and (d) iron(II) concentration. Results are shown for the base conditions in which linoleic acid is the electron donor. For f_{min} = 1.0, there is negligible iron oxide dissolution and therefore negligible iron sulfide precipitation and concentration of iron(II).